A Novel Micro Flow-Focusing Device for the Control of Droplet Contents

Jean Berthier[*1], Jayesh Wagh[2]

CEA-Leti-Minatec, Division of Technology for Life Sciences and Health Care, 17, avenue des Martyrs, 38054 Grenoble, France

[*1]jean.berthier@cea.fr; [2]jayesh.wagh@epfl.ch

***Abstract*- Micro flow-focusing devices (mFFDs) have been used extensively to produce emulsions and for the on-line encapsulation of biologic objects, such as bacteria and cells. More recently, new designs of this type of instrument have been imagined, for example to produce multi-layered capsules. In this work, we present a novel design of mFFD that comprises "moustaches", i.e. escape microchannels, just upstream of the orifice. In the context of encapsulation, such a design authorizes the control of the number of biologic objects imprisoned in a single capsule, and avoids the emission of empty capsules. We have denoted this new type of FFD by the abbreviation EFFD, for "Escape FFD". We first present the concept of the system, then we derive the pressure conditions for the proper functioning of the device, and finally we present an experimental realization.**

Keywords- Flow-Focusing Device; Encapsulation; Meniscus Stability; Interface Breakup; Escape Channels

I. INTRODUCTION

In the modern approach of microfluidics, the use of individual droplets has been constantly increasing. Droplet and digital microfluidics are now essential tools in many domains such as biotechnology and material sciences [1, 2]. Manipulation of single droplets has seen recently many developments [3, 4]. In this work we present a new concept of micro flow-focusing device for a better control of encapsulation process.

Micro flow-focusing devices (mFFDs) have been used extensively to produce emulsions, to perform in-drop chemical reactions, or for the on-line encapsulation of biologic objects, such as bacteria and cells [5-7]. The topic has been abundantly reported in the Literature [8], and some applications are now commercialized [9]. In such devices, a microflow is dispersed into droplets at the contact of an immiscible secondary flow. This microflow is called the dispersed phase because it is later dispersed in droplets, and the secondary flow, the continuous phase that will transport the droplets. The principle is to use "controlled instabilities". This term might seem to be an oxymoron, but the paradox can be easily be explained: on one hand, the instabilities are pertaining to the Plateau-Rayleigh type of instabilities that break a microfluidic jet into droplets; on the other hand, geometrical constraints are used to control the jet breakup. Figure 1 shows the controlled breakup of an aqueous alginate microflow in a mFFD.

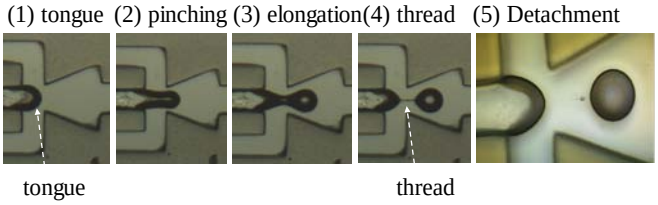

Fig. 1 Controlled droplet formation in a mFFD. The incoming phase (at the middle) is cut in droplets by the action of a second immiscible liquid called the continuous phase (photo P. Dalle, CEA-Leti)

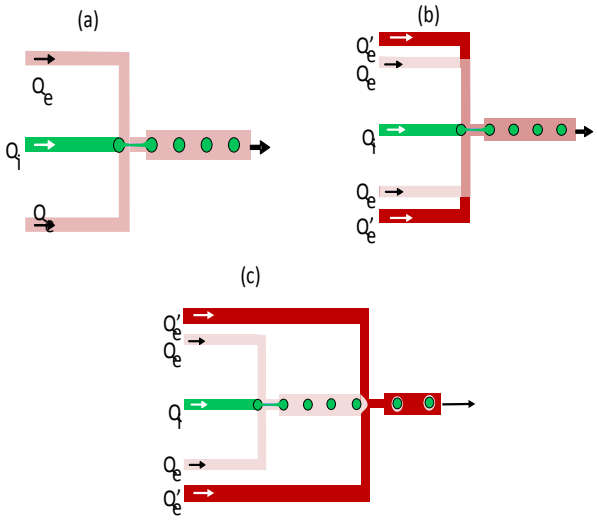

Fig. 2 (a) Conventional FFD; (b) 5-branch FFD; (c) double-FFD

For encapsulation applications, the particles, or cells, etc., are transported by the dispersed phase. When droplets form, they are engulfed or encapsulated in the droplets. Live cells, bacteria, spores have been encapsulated in such devices. More recently investigations have been performed to make the concept more versatile. An example is furnished in Figure 2 where "multi-branched" FFD has been developed to perform specific tasks. By instance the device of Figure 2.b can be used to add gelling agent to the incoming oil phase for the gelation of the shell [10] while Figure 2.c is a double-FFD used for a double-layer encapsulation [11-14].

From the encapsulation standpoint, there is a definite need for controlling the contents encapsulated in a droplet. It has been observed that many capsules are produced empty, with no content in them, just because the transported particles are randomly dispersed in the incoming microflow.

All the empty capsules must be discarded later by a sorting process. It is a time consuming process, not compatible with an integrated system. Hence, researchers have started investigations on this problem; they have focused on the ordering of the transported objects upstream of the device. For example, Edd and colleagues have searched the geometrical conditions in the injection channel to order the particles [15]. On the other hand, because encapsulation is often performed in polymeric solutions, such as alginates or other polysaccharides, Nam and colleagues, and D'Avino and colleagues have searched the conditions for alignment in a viscoelastic microflow [16, 17]. But these solutions are difficult to integrate in a microdevice, because they require a very long upstream channel to achieve ordering of the particles, they also require very precise flow rate conditions.

In this work, we have designed a new passive concept where a droplet is formed only if there is content present, suppressing the formation of empty droplets. It is based on the possibility of the incoming dispersed phase to escape upstream from the junction (orifice), hence the name EFFD, for "escape FFD". It is a passive system, not requiring additional energy source, such as electrical power or acoustic source.

We first present the concept of the system, then we derive the pressure conditions for a proper functioning of the device, and finally we present an experimental realization.

II. THE CONCEPT OF EFFD

The principle is to authorize the dispersed phase—the phase which is later dispersed into droplets—to escape in side "moustaches" or "escape paths" just upstream of the orifice, as shown in Figure 3. These moustaches have a small orifice and are placed as close as possible from the orifice. In absence of particles transported by the dispersed phase—i.e. the dispersed phase is a homogeneous liquid—a meniscus remains stable at the orifice at least when the pressure (or flow rate) conditions are adequately chosen. No drop is then produced. Note that the stability of the meniscus requires very stable hydrodynamic conditions, and very-stable, pressure-actuated micropumps are a preferred solution.

A sufficiently large incoming particle cannot escape through the moustaches because their orifice is small. It is trapped in the vicinity of the meniscus. In our original concept [18], it was expected that a large particle—of diameter comparable to the inner dimensions of the channel— trapped at the interface, will restrict the section available for the escape flow at the moustache orifice; the pressure at the meniscus then increases, until the meniscus breaks and a droplet containing the particle is released. After our experimental investigations, the phenomena appeared to be more complex because the system also works for smaller particles. Probably—this is what we infer from the experimental results—the dynamic pressure on the droplet contributes to the deformation of the stable interface, making it bulge and leading to its breakup.

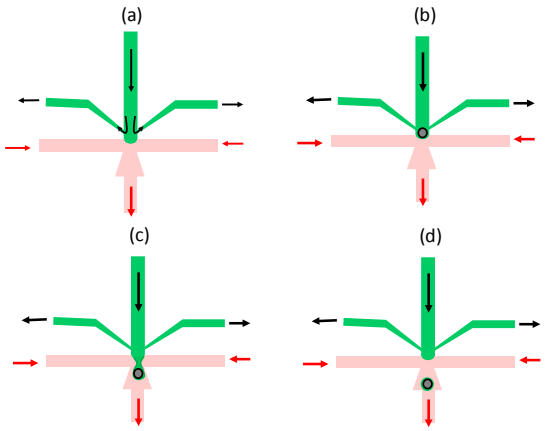

Fig. 3 Sketch of the functioning of the device: (a) in absence of transported object, a meniscus remains stable at the orifice; (b) an incoming large particle is trapped in the vicinity of the interface; (c) an overpressure builds up and the interface breaks; (d) a droplet containing the particle is released and the meniscus pins again at the orifice

The concept has even been extended to a device using a few pairs of moustaches (Fig. 4). In this conceptual design, it is expected that two or more spherical particles will be expelled together, as will be discussed in Section V.

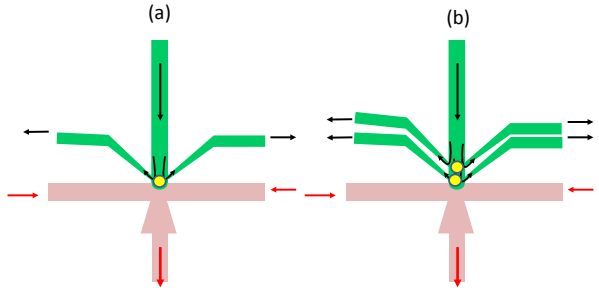

Fig. 4 Sketch of an EFFD: (a) with one pair of moustaches; (b) with two pairs of moustaches

The principle is based on the possibility to obtain a stable meniscus. Experimentally it is very difficult to determine the adequate inlet pressures range. Thus, a theoretical approach has been developed. In the following section, we derive the hydrodynamic conditions for obtaining a stable interface in absence of any incoming particle.

III. MENISCUS STABILITY

In this section we investigate the hydrodynamic conditions before the arrival of a particle, for which a stable meniscus is observed. In this approach, Newtonian fluids are considered. The calculation, however, can be done in a similar, but more complicated approach for non-Newtonian visco-elastic fluids which are often used as the dispersed phase. The derivation of the hydrodynamic conditions for non-Newtonian fluids can be found in Appendix A, and we consider here Newtonian fluids.

An interface pinned at its two ends is stable when the pressure difference across the meniscus does not exceed the Laplace pressure [19]. Let us first calculate the pressure in each channel. In the laminar approach, the general formula

for the pressure drop of a Newtonian fluid, in a channel of hydraulic resistance R is [20, 21]

$$\Delta P = R Q . \quad (1)$$

The value of R for rectangular channel is presented in Appendix B. Hence, the total pressure drop in a complete channel, from inlet to outlet, is

$$P_{in} = \sum_j R_j Q \quad (2)$$

where the index j denotes all the different sections of the network affected by the flow rate Q , and P_{in} is the inlet pressure. The outlet pressure is the atmospheric pressure and has been set to zero for simplicity.

Consider first the continuous phase circuit (index e), where the upstream flow rates are Q_e. The pressure at the interface in the oil phase is then

$$P_{men,e} = 2 \sum R_{downstream,e} \; Q_e \quad (3)$$

where $P_{men,e}$ is the pressure at the meniscus in the oil phase, and the coefficient 2 corresponds to the double flow rate 2 Q_e, downstream from the meniscus. On the other hand, the total pressure drop in the oil phase is

$$\begin{aligned} P_{in,e} &= \sum R_{upstream,e} \; Q_e + 2 \sum R_{downstream,e} \; Q_e \\ &= \sum \left(R_{upstream,e} + 2 R_{downstream,e} \right) Q_e \end{aligned} \quad (4)$$

Combination of (3) and (4) yields

$$\frac{P_{men,e}}{P_{in,e}} = \frac{2 \sum R_{downstream,e}}{\sum \left(R_{upstream,e} + 2 R_{downstream,e} \right)} . \quad (5)$$

Using the same arguments for the dispersed phase, it can easily be shown that

$$\frac{P_{men,i}}{P_{in,i}} = \frac{\frac{1}{2} \sum R_{downstream,i}}{\sum \left(R_{upstream,i} + \frac{1}{2} R_{downstream,i} \right)} \quad (6)$$

where the coefficient ½ stems from the fact that there are two symmetrical moustaches, so that the flow rate Q_i is divided in two at the moustaches' orifice.

Finally, using (5) and (6),

$$\begin{aligned} P_{men,i} - P_{men,e} = & \\ & \frac{\frac{1}{2} \sum R_{downstream,i}}{\sum \left(R_{upstream,i} + \frac{1}{2} R_{downstream,i} \right)} P_{in,i} \\ & - \frac{2 \sum R_{downstream,e}}{\sum \left(R_{upstream,e} + 2 R_{downstream,e} \right)} P_{in,e} \end{aligned} \quad (7)$$

Using Laplace theorem, this pressure difference must not exceed

$$P_{men,i} - P_{men,e} = \gamma \left(\frac{1}{R_h} + \frac{1}{R_v} \right) . \quad (8)$$

where R_h and R_v are the horizontal and vertical minimum curvature radii of the meniscus, and γ the water-oil surface tension. Using the approximations $R_h \sim w/2$ and $R_v \sim d/2$, where w and d are respectively the width and depth of the channel [15], relation (8) becomes

$$P_{men,i} - P_{men,e} \approx \gamma \left(\frac{1}{w/2} + \frac{1}{d/2} \right) . \quad (9)$$

Let us assume for simplicity that the orifices of the moustaches are perfect (ideal case) and that the contact angle is 90°. The meniscus is stable if

$$0 \le P_{men,i} - P_{men,e} \le 2 \gamma \left(\frac{1}{w} + \frac{1}{d} \right) . \quad (10)$$

In reality, in order to obtain aqueous droplets in an organic phase, the channels are silanized, and the contact angle is closer to 100-105° (Fig. 5). In this case, relation (10) must be corrected by

$$2 \gamma \sin\left(\theta - \frac{\pi}{2} \right) \left(\frac{1}{w} + \frac{1}{d} \right) < P_{men,i} - P_{men,e} < 2 \gamma \left(\frac{1}{w} + \frac{1}{d} \right) \quad (11)$$

Note that (11) collapses to (10) for θ=90°. Let us note

$$\alpha = \frac{\frac{1}{2} \sum R_{downstream,i}}{\sum \left(R_{upstream,i} + \frac{1}{2} R_{downstream,i} \right)} , \quad (12)$$

and

$$\beta = \frac{2 \sum R_{downstream,e}}{\sum \left(R_{upstream,e} + 2 R_{downstream,e} \right)} . \quad (13)$$

Then, combining (7) and (11) yields the conditions

$$\begin{aligned} \frac{2\gamma}{\alpha} \sin\left(\theta - \frac{\pi}{2} \right) \left(\frac{1}{w} + \frac{1}{d} \right) + \frac{\beta}{\alpha} P_{in,e} < P_{in,i} & \\ < \frac{2\gamma}{\alpha} \left(\frac{1}{w} + \frac{1}{d} \right) + \frac{\beta}{\alpha} P_{in,e} & \end{aligned} \quad (14)$$

This condition has been graphically represented in Figure 6. The meniscus stability region is the diagonal band in the figure. For the dimensions w=d=150 µm, and γ~40 mN/m, and an approximate value θ~0.8, the width of the stability band is approximately $\frac{2\gamma}{\alpha} \left(\frac{1}{w} + \frac{1}{d} \right)$~1500 Pa. Note that the width of the stability band depends only on θ, not on γ. This sensitivity is obtainable using high precision micropumps (for example Fluigent®).

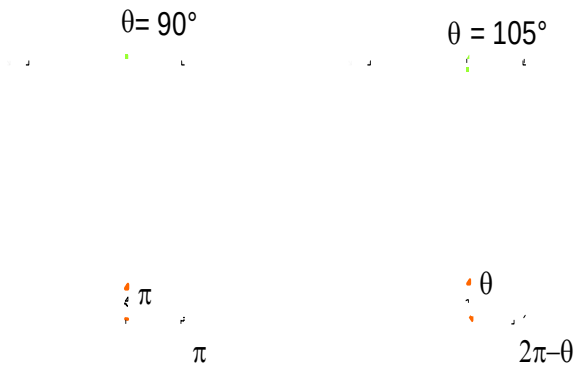

Fig. 5 Sketch of the two limit locations of the pinned interface for a two-dimensional case: (left) for a contact angle of 90°, the lower limit is a flat interface and the upper limit a ½ circle; (right) for a contact angle of 105°, the upper limit is still a ½ circle, but the lower limit is slightly bulging. Below the lower limit the meniscus recedes inside the channel

IV. EXPERIMENTAL RESULTS

Due to the strict constraints on the geometry, the device has been fabricated in silicon. Conventional DRIE etching has been used, and a glass cover is sealed on top of the system. The dimensions of our first system are shown in Figure 7. The moustache orifice being 30 µm, and the width and depth of the channels being w=d=150 µm, it is expected that the system will work for particles between 30 and 150 µm.

Figure 8 shows the trapping of a hollow glass sphere followed by its expulsion inside a droplet. The dispersed phase is water and the continuous phase is mineral oil.

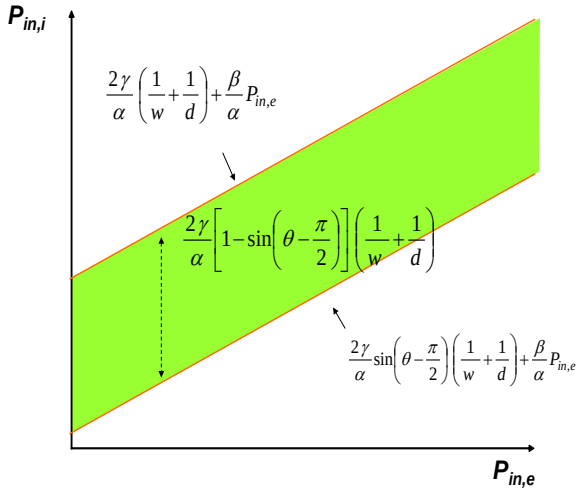

Fig. 6 Stability diagram for the meniscus: the meniscus is stable when point corresponding to the inlet pressures is located in the diagonal band

The sketch of a particle trapped at the interface is shown in Figure 9. The particle and the droplet have been underlined, but the original movie can be found in the ESI.

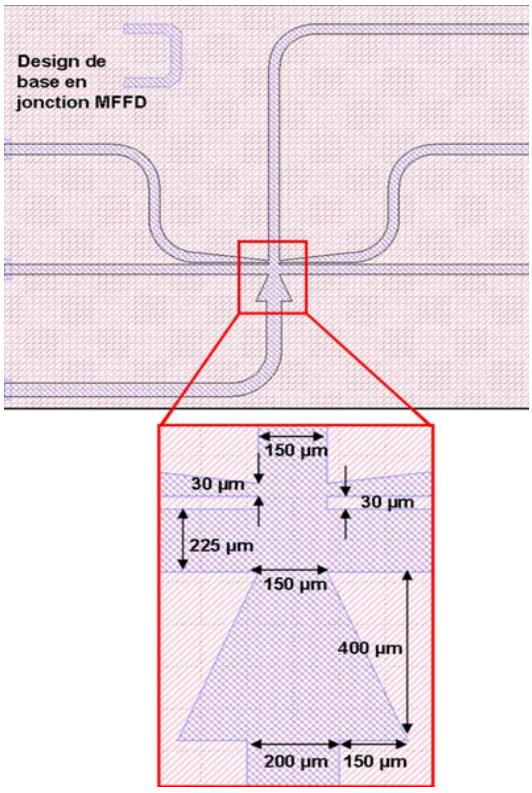

Fig. 7 Lithographic mask of the EFFD device

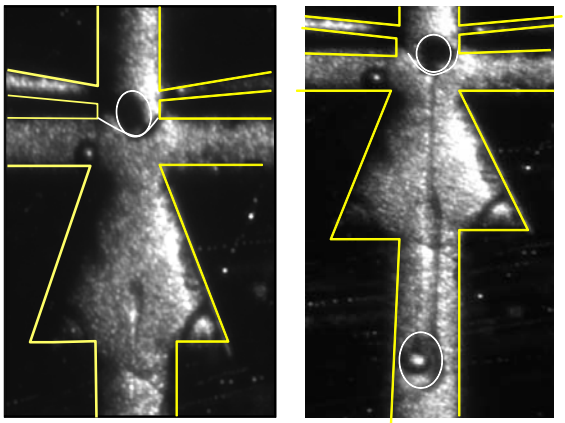

Fig. 8 Left: a hollow glass sphere of 50 µm diameter arrives at the water-oil interface; right: the droplet is expelled while a new sphere arrives at the interface

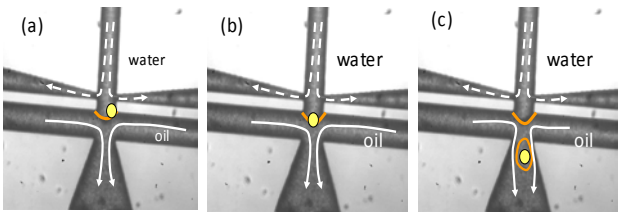

Fig. 9 Left: a hollow glass sphere arrives at the water-oil interface; right: the droplet is expelled while a new sphere arrives at the interface

V. DISCUSSION AND CONCLUSION

The detailed physical mechanisms leading to the droplet formation is not yet fully understood. We are expecting that the particles gathering at the interface would contribute to increase the pressure at the interface by clogging the moustaches. The principle is shown in Figure 10 where the results of a finite element model (COMSOL [22]) show the increase of velocity at the moustache orifice and an increase of the pressure on the sphere. In the calculation, the interface is supposed rigid, in order to avoid the complex problem of a two-phase flow with a moving spherical object. The pressure increases considerably upstream from the sphere and a downwards force is exerted on the sphere. If this force is larger than that of Condition (11), the interface breaks and a droplet containing the sphere is expelled.

Similar calculation can be done for two or more spherical particles showing a larger increase of the pressure with the number of trapped particles (Fig.11). It can also be performed in the case of two pairs of moustaches.

On the other hand, the experiments have shown that the device works with smaller particles which clog much less the moustaches. In such a case, we believe that it is the dynamic pressure on the particles that drives the expulsion of the particle with the droplet, combined to a capillary effect [3]. This is what appears in the movies from the ESI.

Encapsulation is a vast domain. It encompasses biologic applications as well as material sciences applications. In the first case, the objects to encapsulate are most of the time deformable, aqueous-based objects, such as cells and bacteria. In the second case, the capsule content is often rigid, such as solid beads or shells. So far our experiments have used only rigid polystyrene or glass spheres. It is not yet known how deformable biologic objects will behave in the system. This is an important point that needs to be further investigated.

In the future, it would also be of interest to investigate whether multi-FFD systems, such as the one sketched in Figure 2.c, can be implemented with EFFDs in series. At a first sight, it seems possible to obtain stable interfaces when no particle circulates in the system. However, the remaining question is whether a droplet released at the first EFFD will trigger instantaneous interface instability in the second EFFD, leading to the emission of an empty droplet.

In conclusion, in this work, a novel flow-focusing device (EFFD), using escape channels or moustaches at the dispersed phase flow orifice, has been presented. It automatically suppresses the formation of droplets without particulate content. Droplets form only at the arrival of one or more particles. More study is needed to determine the best conditions for the encapsulation of one particle at the time, and to investigate the behavior of deformable objects.

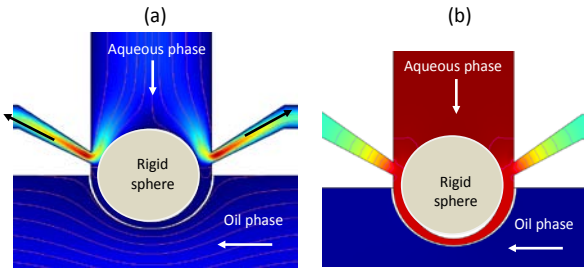

Fig. 10 COMSOL finite element model for the velocity field (a) and the pressure field (b) in the vicinity of the interface when a large particle restricts the escape channels (moustaches)

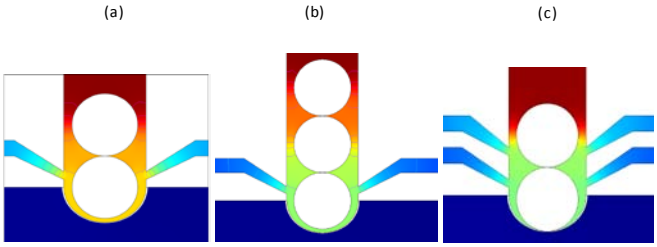

Fig. 11 Pressure field for an EFFD: (a) two spherical particles; (b) three spherical particles; (c) EFFD with two pairs of moustaches

ACKNOWLEDGMENT

We would like to thank Prisca Dalle for the photographs of Figure 1 and Raphaël Renaudot for the lithography mask of Figure 7.

REFERENCES

[1] Shia-Yen Teh, R. Lin, Lung-Hsin Hung and A. P. Lee, "Droplet microfluidics," *Lab Chip*, Vol. 8, pp.198-220, 2008.

[2] F. Mügele, J-C Baret, "Electrowetting: fropm basics to applications," *J. Phys: Condens. Matter*, Vol. 17, p. R705-R774, 2005.

[3] J. Berthier, K. Brakke, "*The physics of microdroplets*," Scrivener-Wiley Publishing, 2012.

[4] Ziqian Wang, Feng-Chao Wang, Ya-Pu Zhao, "Tap dance of water droplet," *Proc. R. Soc. A*, Vol. 468, n° 2145, pp. 2485-2495, 2012.

[5] E. Kumacheva, P. Garstecki, "*Microfluidic reactors for polymer particles*," Wiley Publishing, March, 2011.

[6] B. Franz, S.S. Balkundi, C. Dahl, Y.M. Lvov, A. Prange, "Layer-by-Layer Nano-Encapsulation of Microbes: Controlled Cell Surface Modification and Investigation of Substrate Uptake in Bacteria," *Macromolecular Bioscience*, Vol. 10, n°2, pp. 164–172, 2010.

[7] V. L. Workman, S. B. Dunnett, P. Kille, D. D. Palmer, "Microfluidic chip-based synthesis of alginate microspheres for encapsulation of immortalized human cells," *Biomicrofluidics*, Vol. 1, p. 014105, 2007.

[8] R. Gugerli, "Polyelectrolyte-complex and covalent –complex microcapsules for the encapsulation of mammalian cells: potential and limitations," Ph.D. Dissertation at Ecole Polytechnique Fédérale de Lausanne, n°2720, 2003.

[9] RainDance Technologies: http://www.raindancetech.com/

[10] V. L. Workman, S. B. Dunnett, P. Kille, D. D. Palmer, "On-Chip Alginate Microencapsulation of Functional Cells," *Macromol. Rapid Commun*. Vol. 29, pp. 165–170, 2008.

[11] Zigang Yang, Fen Zhou, Jianjun Yuan, Lixin Ma, Chao Zhai, Shiyuan Chang, "Preparation of PLL-PEG-PLL and its application to DNA encapsulation," *Science in China, Series B: Chemistry*, Vol. 49, n°4, pp. 357-362, 2006.

[12] J. Berthier, "*Microdrops and digital microfluidics*," William-Andrew Publishing, 2008.

[13] H. Gu, M.H.G. Duits, F. Mugele, "Droplets formation and merging in two-phase flow microfluidics," *Int. J. Mol. Sci*., Vol. 12, pp. 2572-2597, 2011.

[14] Shin-Hyun Kim, Jin Woong Kim, Jun-Cheol Cho and D. A. Weitz, "Double-emulsion drops with ultra-thin shells for capsule templates," *Lab Chip*, Vol. 11, p. 3162, 2011.

[15] J. F. Edd, D. Di Carlo, K. J. Humphry, *S.* Köster, D. Irimia, D. A. Weitz and M. Toner, "Controlled encapsulation of single-cells into monodisperse picolitre drops," *Lab-Chip*, Vol.8, pp. 1262-1264, 2008.

[16] J. Nam, H. Lim, D. Kim, H. Jung, S. Shin, "Continuous separation of microparticles in a microfluidic channel via the elasto-inertial effect of non-Newtonian fluid," *Lab Chip*, Vol. 12, p. 1347, 2012.

[17] G. D'Avino, G. Romeo, M.M. Villone, F. Greco, P.A. Netti, P.L. Maffettone, "Single line particle focusing induced by viscoelasticity of the suspending liquid: theory, experiments and simulations to design a micropipe flow-focuser," *Lab Chip*, Vol. 12, pp. 1638-1645, 2012.

[18] J. Berthier, S. Le Vot, et F. Rivera, World Patent WO2010146261.

[19] A. W. Adamson, A. P. Gast, "*Physical Chemistry of Surfaces (6th edition)*," Wiley Interscience, 1997.

[20] J. Berthier, P. Silberzan, "*Microfluidics for Biotechnology*," Second Edition. Artech House, 2010.

[21] H. Bruus, "*Theoretical microfluidics*," Oxford University Press, 2007.

[22] COMSOL numerical software: http://www.comsol.com

[23] G. W. Scott Blair, J. C. Hening , A. Wagstaff , "The Flow of Cream through Narrow Glass Tubes," *J. Phys. Chem*., Vol. 43, n° 7, pp. 853–864, 1939.

[24] J.F. Steffe, "*Rheological methods in food process engineering*," Second Edition, Freeman Press, 1982.

[25] Y.S. Muzychka, J.F. Edge, "Laminar non-Newtonian fluid flow in non-circular ducts and microchannels," *J. Fluid Engineering*, Vol. 130, n°11, p. 111-201, 2008.

[26] C. Miller, "Predicting non-Newtonian flow behaviour in ducts of unusual cross section," *Ind. Eng. Chem. Fundam*., Vol.11, pp. 534–628, 1972.

[27] F. Delplace, J.C. Leuliet, "Generalized Reynolds number for the flow of power law fluids in cylindrical ducts of arbitrary cross-section," *Chem.Eng. Journal*, Vol. 56, pp.33-37, 1995.

[28] W. Kosicki, C.H. Chou, C. Tiu, "Non-Newtonian Flow in Ducts of Arbitrary Cross-sectional Shape," *Chemical Engineering* Science, Vol. 21, pp. 665–679, 1996.

[29] M. Bahrami, M. M. Yovanovich, J. R. Culham, "Pressure drop of fully-developed, laminar flow in microchannels of arbitrary cross section," *Proceedings of ICMM 2005, 3rd International Conference on Microchannels and Minichannels*, June 13-15, 2005, Toronto, Ontario, Canada, 2005.

APPENDIX A: NON-NEWTONIAN APPROACH

In the (frequent) case of a « power-law » or Waele-Ostwald fluid [23], the fluid viscosity can be expressed by

$$\eta = \frac{\tau}{\dot{\gamma}} = K\,\dot{\gamma}^{\,n-1} \tag{15}$$

where K and n are coefficients depending on the concentration in polymers, and $\dot{\gamma}$ the shear rate. For example, in the case of a 1.25 wt% Keltone alginate concentration, K=0.5 and n=0.8. For cylindrical channels Rabinowitsch and Mooney have derived a closed form expression for the pressure drop [24,25]

$$\Delta P = \frac{2\,L\,K\,U^n}{r^{n+1}}\left(\frac{3n+1}{n}\right)^n = \frac{2\,L\,K}{\pi^n r^{3n+1}}\left(\frac{3n+1}{n}\right)^n Q^n \tag{16}$$

where L is the length of the cylinder and r its radius. We can define a hydraulic resistance by

$$R = \frac{\Delta P}{Q} = \frac{2\,L\,K}{\pi^n\, r^{3n+1}}\left(\frac{3n+1}{n}\right)^n Q^{n-1} \tag{17}$$

To the difference with the Newtonian case, the hydraulic resistance depends on the flow rate. For rectangular channels, the pressure drop can be approximated by [26-28]

$$\Delta P = \frac{K\,L}{D_h}\frac{1}{(w\,d)^{\frac{3n}{2}}}\,2^{n+2}\left(\frac{c_1}{n}+c_2\right)^n\left(\frac{2(\varepsilon+1)}{\sqrt{\varepsilon}}\right)^n Q^n \tag{18}$$

where D is the hydraulic diameter $D = \dfrac{2\,w\,d}{w+d}$ and □ the aspect ratio $\varepsilon = \min\left(\dfrac{w}{d},\dfrac{d}{w}\right)$. The constants c_1 and c_2 are given by

$$c_1 = \frac{1}{2(1+\varepsilon)^2\left(1-\dfrac{32}{\pi^3\cosh\left(\dfrac{\pi}{2\varepsilon}\right)}\right)}$$
$$c_2 = \frac{3}{2(1+\varepsilon)^2\left(1-\dfrac{192\,\varepsilon\tanh\left(\dfrac{\pi}{2\varepsilon}\right)}{\pi^5}\right)} - c_1 \tag{19}$$

The hydraulic resistance is then

$$R = \frac{\Delta P}{Q} = \frac{K\,L}{D}\frac{1}{(w\,d)^{\frac{3n}{2}}}\,2^{n+2}\left(\frac{c_1}{n}+c_2\right)^n\left(\frac{2(1+\varepsilon)}{\sqrt{\varepsilon}}\right)^n Q^{n-1} \tag{20}$$

We can then write

$$P_{in} = \sum_j R_j\,Q = K\sum_j R_j^*\,Q^n \tag{21}$$

where

$$R_j^* = f\left(D_j, w_j, d_j, L_j, n\right)$$
$$= \frac{L_j}{D_j}\frac{1}{(w_j\,d_j)^{\frac{3n}{2}}}\,2^{n+2}\left(\frac{c_{1,j}}{n}+c_{2,j}\right)^n\left(\frac{2(1+\varepsilon_j)}{\sqrt{\varepsilon_j}}\right).$$

The coefficient R_j^* depends on the geometry and on the exponent n. The pressure at the meniscus is then given by

$$\frac{P_{men}}{P_{in}} = \frac{KQ^n \sum_{j\in downstream} R_j^*}{KQ^n \sum_{j\in all} R_j^*} = \frac{\sum_{j\in downstream} R_j^*}{\sum_{j\in all} R_j^*} \quad (22)$$

This expression is very similar to that found for Newtonian fluids (6); the difference stems from the expressions of the hydraulic resistances. Note that only one of the two coefficients of the viscoelastic rheology appears in (22): the exponent n is present in (22) while K is absent.

APPENDIX B: HYDRAULIC RESISTANCE OF NEWTONIAN FLUIDS IN RECTANGULAR MICROCHANNELS

There exist a few expressions for the hydraulic resistance of a square microchannel [20,21]. We have tested with success the one from Barhami and colleagues [29]

$$R = \frac{8\eta L}{w d \min(d,w)^2 \chi}, \quad (23)$$

where w, d and L are respectively the width, depth and length of the channel, η the dynamic viscosity, and χ an aspect ratio factor. This function can be expressed by

$$\chi = 2\left(\frac{1}{3} - \frac{64\,\varepsilon}{\pi^5}\tanh\frac{\pi}{2\,\varepsilon}\right) \quad (24)$$

where ε is the aspect ratio: $\varepsilon = \min(w/d, d/w)$.

Jean Berthier is a Scientist at the CEA Leti and teaches at the University of Grenoble France. He received an Engineering Diploma from the Institut National Polytechnique, Grenoble, France, a MS in Mathematics from the University of Grenoble and a PhD from the University Pierre and Marie Curie / Sorbonne, Paris. He is presently involved in the development of microdevices for liquid-liquid extraction (LLE), flow focusing devices (FFD) for bio-encapsulation of live cells, microfluidic resonators for high sensitivity biodetection and theoretical and numerical methods for the prediction of droplets and interfaces behavior in microsystems. He is the first author of the book *Microfluidics for Biotechnology* first published by Artech House in November 2005, with a second edition in 2010. He is also the author of the book *Microdrops and Digital Microfluidics* published by William Andrew/Elsevier in February 2008 and the first author of *The Physics of Microdroplets* published by Scrivener-Wiley in May 2012. He is a member of the editorial board of the journals Biomicrofluidics and Modern Instrumentation, a member of the American Chemical Society, and of the French Observatory for Micro and Nano Technology (OMNT). He has published numerous scientific papers and patents.

Jayesh Wagh received his Bachelor degree in Biomedical Engineering from University of Mumbai, India in 2009. He received his Masters in Nanoscale Engineering from Ecole Centrale de Lyon, France in 2012. He pursued in 2011an internship at CEA-Leti on droplet microfluidics, and in 2012 at EPFL on 3D cell culture. His current research interest includes droplet microfluidics, bio MEMS, lab-on-chips and micro fabrication methods.